European Journal of Pharmaceutics and Biopharmaceutics 144 (2019) 79–90

Contents lists available at ScienceDirect

European Journal of Pharmaceutics and Biopharmaceutics

journal homepage: www.elsevier.com/locate/ejpb

Comparative study of the potential of poly(2-ethyl-2-oxazoline) as carrier in the formulation of amorphous solid dispersions of poorly soluble drugs

Eline Boel[a], Annelies Smeets[a], Maarten Vergaelen[b], Victor R. De la Rosa[b], Richard Hoogenboom[b], Guy Van den Mooter[a,*]

[a] KU Leuven, Department of Pharmaceutical and Pharmacological Sciences, Drug Delivery and Disposition, 3000 Leuven, Belgium
[b] Supramolecular Chemistry Group, Centre of Macromolecular Chemistry (CMaC), Department Organic and Macromolecular Chemistry, Ghent University, Krijgslaan 281-S4, 9000 Gent, Belgium

ARTICLE INFO

Keywords:
Amorphous solid dispersion
Poly(2-ethyl-2-oxazoline)
Spray drying
Hot melt extrusion
Cryo-milling

ABSTRACT

Despite the fact that solid dispersions are gaining momentum, the number of polymers that have been used as a carrier during the past 50 years is rather limited. Recently, the poly(2-alkyl-2-oxazoline) (PAOx) polymer class profiled itself as a versatile platform for a wide variety of applications in drug delivery, including their use as amorphous solid dispersion (ASD) carrier. The aim of this study was to investigate the potential of poly(2-ethyl-2-oxazoline) (PEtOx) by applying a benchmark approach with well-known, commercially available carriers (*i.e.* polyvinylpyrrolidone (PVP) K30, poly(vinylpyrrolidone-co-vinyl acetate) (PVP-VA) 64 and hydroxypropylmethylcellulose (HPMC)). For this purpose, itraconazole (ITC) and fenofibrate (FFB) were selected as poorly water-soluble model drugs. The four polymers were compared by establishing their supersaturation maintaining potential and by investigating their capability as carrier for ASDs with high drug loadings. Spray drying, as well as hot melt extrusion and cryo-milling were implemented as ASD manufacturing technologies for comparative evaluation. For each manufacturing technique, the formulations with the highest possible drug loadings were tested with respect to *in vitro* drug release kinetics. This study indicates that PEtOx is able to maintain supersaturation of the drugs to a similar extent as the commercially available polymers and that ASDs with comparable drug loadings can be manufactured. The results of the *in vitro* dissolution tests reveal that high drug release can be obtained for PEtOx formulations. Overall, proof-of-concept is provided for the potential of PEtOx for drug formulation purposes.

1. Introduction

Since the early nineties, drug selection procedures have experienced dramatic changes, driven by the advent of rational drug design strategies like high throughput screening and combinatorial chemistry. These procedures often lead to new drug candidates that tend to have a high affinity and selectivity for their biological targets but on the other hand imply discovery of drug candidates with unfavourable properties, in particular low aqueous solubility and consequently low bioavailability after oral administration [1,2]. Most of these drugs are therefore classified as BCS (Biopharmaceutics Classification System) class II compounds, which are characterized by low solubility and high permeability and, hence, their dissolution rate and solubility are the rate limiting steps in oral absorption. The evolution towards these new drug candidates with low aqueous solubility is evidenced by the shift in the share of BCS class II drugs from 33% of marketed drugs towards 54% of new chemical entities [3]. This means that currently more than 50% of newly developed drug compounds need an enabling formulation strategy, emphasizing the increasing importance of studying innovative drug formulations. Throughout the years, many strategies have been

Abbreviations: API, active pharmaceutical ingredient; ASD, amorphous solid dispersion; AUC, area under the curve; AUC Der. RHF, AUC of the derivative of the reversing heat flow; BCS, Biopharmaceutics Classification System; CM, cryo-milling; DS, degree of supersaturation; FaSSGF, fasted state simulated gastric fluid; FaSSIF, fasted state simulated intestinal fluid; FFB, fenofibrate; HME, hot melt extrusion; HPMC, hydroxypropylmethylcellulose; HPMC-AS, hydroxypropylmethylcellulose acetate succinate; ITC, itraconazole; mDSC, modulated differential scanning calorimetry; PAOx, poly(2-alkyl-2-oxazoline)s; PEtOx, poly(2-ethyl-2-oxazoline); PMeOx, poly(2-methyl-2-oxazoline); PVP, polyvinylpyrrolidone; PVP-VA, poly(vinylpyrrolidone-co-vinyl acetate); RHF, reversing heat flow; SD, spray drying; SF, supersaturation factor; T_g, glass transition temperature; THF, total heat flow; Tm, melting temperature; XRPD, X-ray powder diffraction

* Corresponding author at: Department of Pharmaceutical and Pharmacological Sciences, Drug Delivery and Disposition, KU Leuven, O&N2 Herestraat 49 Bus 921, 3000 Leuven, Belgium.
E-mail address: guy.vandenmooter@kuleuven.be (G. Van den Mooter).

https://doi.org/10.1016/j.ejpb.2019.09.005
Received 20 June 2019; Received in revised form 8 August 2019; Accepted 6 September 2019
Available online 06 September 2019
0939-6411/

developed to formulate BCS class II compounds with a view to overcome poor solubility, including particle size reduction to the nanometer range, formation of water soluble complexes (*e.g.* cyclodextrin complexes), self-emulsifying drug delivery systems, ordered mesoporous silica, co-crystals, co-solvency, salt formation and amorphous solid dispersions (ASDs) [2]. Among them, ASDs offer great potential to tackle low oral bioavailability issues [2,4,5]. Since no lattice energy must be overcome in amorphous materials, the rate and extent of dissolution is improved compared to crystalline materials. However, these amorphous materials also possess a higher Gibbs energy and from a thermodynamic point of view, materials always try to lower their Gibbs energy in order to aspire an increase in total entropy [6]. Amorphous materials are therefore thermodynamically unstable and tend to undergo structural relaxation, nucleation and crystallization. Due to this thermodynamic instability, amorphous drugs can hardly ever be marketed as such [7]. This problem is addressed by molecularly dispersing the poorly soluble drug within an inert polymer matrix ("carrier") in the solid state to create a so-called ASD [4]. The aforementioned thermodynamic instability of the amorphous drug can consequently be avoided due to anti-plasticizing effects of the carrier by increasing the glass transition temperature (T_g) and the creation of a physical barrier related to the higher viscosity of the carrier. Reduction in the chemical potential of the drug and most notably inter-molecular interactions with the carrier such as hydrogen bonds also play a key role in the physical stability of ASDs. Moreover, the carrier must be able to install and maintain supersaturation of the drug in the gastrointestinal tract in order to reach an adequate driving force for absorption [8,9].

ASDs can be prepared in a variety of ways, namely by rapid cooling of a melt, precipitation of a drug-carrier solution or by direct solid conversion methods. These can be classified as heat-based methods, solvent-based methods and mechanochemical-based methods, respectively [10]. Because different preparation methods entail altered final product properties, an adequate rational selection of a manufacturing technology is indispensable [7]. Heat-based methods apply the principle of rapid cooling of a melt as amorphization procedure and encompass spray congealing, melt granulation and hot-melt extrusion (HME). Such heat-based methods are only reliable for thermostable drugs but are of utmost importance regarding upscaling and continuous manufacturing purposes [7]. Solvent-based methods use the intermediate step of a solution to convert the crystalline material into the amorphous state. Examples of these methods are film casting, bead coating, co-precipitation, freeze drying, electrospraying and spray drying [4]. A huge benefit over the heat-based methods is that more thermolabile drugs can be processed. Nonetheless, one must be aware of the drawbacks associated with the use of solvents with respect to potential toxicological and environmental issues. Mechanochemical activation (*e.g.* cryo-milling), which is a direct solid conversion technique, can also be used to prepare ASDs, but is still considered as non-conventional [11].

Despite the fact that solid dispersions are gaining momentum, the number of polymers that have been used as a carrier for ASDs during the past 50 years is rather limited [12]. Furthermore, there is currently a constrained number of 24 solid dispersion formulations marketed over a period of 30 years, which may be due to large-scale manufacturing difficulties and physical stability issues [8,13]. In addition, this limited market share may also be linked to disadvantages associated with currently available polymer carriers. The few carrier options that formulation specialists have for screening purposes can pose problems regarding stability and processability. Moreover, no carrier structure is so versatile that it can serve as a platform for the formulation of a broad range of active pharmaceutical ingredients (APIs) [6]. Regarding these limitations, poly(2-alkyl-2-oxazoline)s (PAOx) are thought-provoking as alternative carriers for drug delivery purposes or in this more specific case for ASDs [14–16]. This polymer class is synthesized by cationic ring opening polymerization (CROP) of 2-substituted 4,5-dihydrooxazoles, referred to as 2-oxazolines [17]. The polymerization of 2-oxazolines allows full control over the polymer molar mass and side-chain composition, enabling the production of materials with a wide range of solubility properties: from superhydrophilic *via* thermoresponsive to superhydrophobic [18]. The introduction of chain-end as well as side-chain functionalities into the polymer structure is as well straightforward [19,20]. Hence, a platform of differently substituted PAOx could be envisioned for the formulation of a wide variety of APIs with different physicochemical properties. Based on subtle structural variations, it may be anticipated that different dissolution properties can be obtained. This tunability of hydrophilicity can be useful to further optimize formulations regarding drug release or to produce immediate as well as sustained release formulations [14]. In addition to structural versatility, processability is a major advantage for this relatively new class of polymers [14,17]. Moreover, PAOx are considered to pose high physical and chemical stability and are proven to be biocompatible [21,22]. Recent publications propose the potential of poly(2-ethyl-2-oxazoline) (PEtOx) (*i.e.* a PAOx with ethyl side-chains) as ASD carrier, namely Claeys et al. investigated the potential of PEtOx as a matrix excipient using HME as manufacturing technology and set forth the possibility of molecularly dispersing a poorly soluble drug within the polymer, thereby enhancing the dissolution rate [14]. The research of Fael et al. certified this aspect using the solvent evaporation method and even stated that PEtOx could serve as an alternative to polyvinylpyrrolidone (PVP) for improving oral bioavailability of poorly water-soluble drugs [15]. However, our research goes beyond merely examining the possibility of preparing ASDs with PEtOx and elaborating the resulting drug solubility enhancing effects. The overall aim of this study is to investigate the potential of PEtOx by applying a benchmark approach, which allows comparison to three well-known, commercially available carriers namely PVP K30, poly(vinylpyrrolidone-co-vinyl acetate) (PVP-VA) 64 and hydroxypropylmethylcellulose (HPMC). For this purpose, we investigate the formation of ASDs with defined PEtOx, in contrast to previous reported studies that used technical grade PEtOx (brand-named Aquazol®), with itraconazole (ITC) and fenofibrate (FFB) as selected BCS class II model drugs. The four polymers were compared by establishing the supersaturation maintaining potential and by elaborating their capability as carrier for ASDs with high drug loadings. Since it is known that different ASD manufacturing techniques will result in different product properties, ASDs were prepared with a heat-based technique (*i.e.* HME), as well as with a solvent-based technique (*i.e.* spray drying) and a mechanochemical activation technique (*i.e.* cryo-milling). For each manufacturing technique, the formulations with the highest possible drug loadings were tested with respect to *in vitro* drug release kinetics. Since the focus lies on the investigation of the potential of PEtOx to form a one phase ASD with a poorly soluble model drug, to evaluate the drug release from these systems and to study the supersaturation maintaining properties, physical stability studies were not within the aim of this research and therefore not conducted.

2. Materials and methods

2.1. Materials

ITC and FFB were obtained from Janssen Pharmaceutica N.V. (Beerse, Belgium) and Hangzhou DayanChem (Hangzhou City, China), respectively. Defined PEtOx with a molar mass of 50,000 g/mol and a dispersity of 1.15 and 25,000 g/mol poly(2-methyl-2-oxazoline) (PMeOx) with a dispersity of 1.34 (measured by Size Exclusion Chromatography against poly(methyl methacrylate) standards) were prepared following our recently published improved synthesis protocol [23]. PVP K30 and PVP-VA 64 were both obtained from BASF® ChemTrade GmbH (Ludwigshafen, Germany) and HPMC 2910 (5 mPa s) was purchased from Colorcon (Dartford, UK).

HCl was purchased from Fisher Scientific U.K. Limited (Loughborough, UK), $NaH_2PO_4{\cdot}H_2O$ from Honeywell (Seelze, Germany)

and Na_2HPO_4 from Sigma-Aldrich GmbH (Steinheim, Germany). Biorelevant.com (Croydon, U.K.) provided FaSSIF/FaSSGF/FeSSIF powder. NaCl and NaOH were supplied by Chemlab N.V. (Zedelgem, Belgium) and Merck (Darmstadt, Germany), respectively. Polytetrafluorethylene (PTFE) filters were obtained from VWR International and dimethylsulfoxide (DMSO) was purchased from ACROS (Geel, Belgium). Fisher Scientific U.K. Limited (Loughborough, UK) supplied acetonitrile (ACN). Acetic acid and sodium acetate were both obtained from VWR Chemicals (Leuven, Belgium). Dichloromethane (DCM), methanol (MeOH), phosphoros pentoxide and $Na_3PO_4{\cdot}12H_2O$ were all acquired from ACROS (Geel, Belgium).

2.2. Solubility and supersaturation experiments

Solubility and supersaturation experiments were carried out in simple as well as in more advanced (more biorelevant) media. Both acidic and neutral media were implemented, given the simulation of the gastro-intestinal tract environment in pharmaceutical performance experiments. HCl 0.1 M and a 20 mM phosphate buffer were used as simple acidic and neutral medium respectively. Biorelevant acidic medium (fasted state simulated gastric fluid - FaSSGF) was obtained by dissolving FaSSIF/FaSSGF/FeSSIF powder (0.060 mg/mL) in 1 L purified water, containing 2 g of NaCl. The pH of this solution was adjusted to 1.6 with 1 M HCl after magnetic stirring for 2 h. To prepare biorelevant neutral medium, consisting of ¼ FaSSGF and ¾ FaSSIF (fasted state simulated intestinal fluid), the latter component was made by dissolving 5.26 mg/ml $NaH_2PO_4{\cdot}H_2O$, 8.23 mg/ml NaCl, 0.56 mg/ml NaOH and 2.99 mg/ml FaSSIF/FaSSGF/FeSSIF powder in purified water. After 2 h of magnetic stirring, the pH was subsequently adjusted to 6.5. In this paper, the term 'biorelevant neutral medium' is often replaced with the term 'FaSSIF'. However, the reader should keep in mind that these terms refer to the mixture of FaSSGF and FaSSIF. The biorelevant media were used for experimental work within 48 h after the preparation.

2.2.1. Solubility experiments

The thermodynamic solubility of ITC and FFB was determined in triplicate in 10 mL glass test tubes using the shake-flask method for 48 h. An excess of API was added to 5 mL aqueous media (both simple and biorelevant media), either in presence or absence of 0.5% (w/V) PVP K30, PVP-VA 64, HPMC, PEtOx or PMeOx. After 48 h, samples were filtered through pre-saturated PTFE filters (0.2 μm) and analysed as such with HPLC.

2.2.2. Supersaturation experiments

The supersaturation behaviour of ITC and FFB was investigated in triplicate by using the solvent-shift method, either in absence or presence of 0.5% (w/V) PVP K30, PVP-VA 64, HPMC, PEtOx or PMeOx (both in simple and biorelevant media), in order to draw conclusions on the precipitation inhibition capacity of the different polymers. Based on the determined equilibrium solubility, 1.0 mL stock solutions of API in DMSO were prepared to obtain a degree of supersaturation (DS) of 20. From these stock solutions, 200 μL were added to glass beakers, containing 19.80 mL media either with or without polymer, which were continuously stirred throughout the experiment. Samples were taken after predetermined timepoints (15, 30, 45, 60 and 120 min), filtered through pre-saturated PTFE filters (0.2 μm) and subsequently diluted threefold with mobile phase for HPLC analysis. Supersaturation factors (SF) for the time range 15–120 min were calculated by using the mean area under the curve (AUC) values, according to the following equation:

$$SF = \frac{\text{AUC } (15-120 \text{ min}) \textit{ supersaturation in presence of polymer}}{\text{AUC } (15-120 \text{ min}) \textit{ solubility in presence of polymer}} \quad (1)$$

Note that (for both solubility and supersaturation experiments) adsorption of ITC and FFB to PTFE filters (0.2 μm) was investigated upfront by HPLC analysis of subsequently filtered fractions of a saturated API solution. This led to the conclusion that, for both ITC and FFB, 10 mL of a saturated API solution (*i.e.* in simple acidic medium) are needed in order to pre-saturate the filters before use.

2.3. High performance liquid chromatography (HPLC)

Quantification of ITC and FFB concentrations was done by HPLC analysis using a VWR HITACHI Chromaster System (consisting of a 5160 pump, a 5260 autosampler, a 5310 column oven and a 5410 UV detector), equipped with a Nucleodur C-18 column (150 mm, 4.6 mm ID, particle size 5 μm) obtained from Macherey-Nagel (Düren, Germany). Data acquisition was performed using Chromaster System Manager Software (version 1.1). An isocratic HPLC-method was developed for both ITC and FFB. In case of ITC, acceptable retention times of approximately 4.5 min and hence run times of 7 min were obtained by using a mobile phase consisting of ACN/25 mM sodium acetate buffer (pH 3.50) in a ratio of 75/25 (V/V), a flow rate of 1 mL/min and 20 μL injection volume. The detection wavelength was set at 262 nm. For FFB, the mobile phase consisted of ACN/25 mM sodium acetate buffer (pH 3.50) in an 85/15 (V/V) ratio, resulting in acceptable retention times (*ca.* 5 min) and run times of 7 min. As for ITC, a flow rate of 1 mL/min and an injection volume of 20 μL were applied, but with the detection wavelength set at 290 nm. These methods were validated for linearity (coefficient of determination $R^2 > 0.995$) and for intra- and inter-day variability. The limit of detection (LOD) and limit of quantification (LOQ) were determined based on signal to noise ratios, resulting in values of 4.8 ng/mL and 16 ng/mL, respectively (*i.e.* for ITC) and values of 5.35 ng/mL and 18 ng/mL, respectively (*i.e.* for FFB).

2.4. ASD manufacturing

2.4.1. Spray drying

Spray dried formulations were prepared with a Büchi mini spray dryer B-191 (Büchi, Flawil, Switzerland). An accurate amount of API and polymer (either PVP K30, PVP-VA 64, HPMC or PEtOx) was dissolved in a binary solvent mixture of DCM:MeOH (1:1, V:V) in order to obtain a solid content of 10% w/V. The drying air temperature in the drying chamber was set at 52 °C, *i.e.* the average of the boiling points of DCM and MeOH (39.6 °C and 64.7 °C, respectively) and the drying air flow rate at 33 m^3/h. The feed solution flow rate was set at 5 mL/min and the atomization air flow rate at 10 L/min. For FFB-PEtOx formulations, the above-described parameters were adapted in order to obtain a powder. In this case, pure DCM was used as solvent and the drying air temperature was set at 35 °C. The feed solution flow rate was halved and the atomization air flow doubled. Immediately after spray drying, the collected ASDs were further dried in a vacuum oven for 72 h at room temperature. Afterwards, the samples were stored at −28 °C in the presence of phosphorus pentoxide until further analysis (*i.e.* solid-state characterization and determination of drug release kinetics).

2.4.2. Hot melt extrusion

Physical mixtures of drug-polymer combinations were prepared with a mortar and pestle and extruded using a Mini extruder, supplied by DSM Xplore (Sittard, The Netherlands). The extruder is a fully intermeshing recirculating 5 cm^3 extruder, consisting out of two co-rotating screws. In case of ITC, the barrel temperature was set at 170 °C, which is above its melting point (T_m) (*i.e.* 168 °C). For the FFB formulations with PEtOx, a barrel temperature of 85 °C was applied, based on the T_m of FFB (*i.e.* 80 °C). For the FFB-PVP-VA, FFB-PVP and FFB-HPMC formulations, a barrel temperature of 10 °C above the T_g of the polymer was applied, being 120 °C, 170 °C and 160 °C, respectively. For every batch, about 5 g was fed into the extruder via the hopper and mixed for 5 min with a screw speed of 100 rpm. The extrudates were collected and cooled on aluminum foil and milled for 3 min using a

laboratory cutter mill (Kika, Staufen, Germany).

The milled extrudates were subsequently sieved (through a 355 μm sieve) and stored at −28 °C in the presence of phosphorus pentoxide until further analysis (*i.e.* solid-state characterization and determination of drug release kinetics).

2.4.3. Cryo-milling

Cryogenic grinding was performed using a CryoMill (Retsch, Düsseldorf, Germany). Physical mixtures of drug-polymer combinations were prepared using a mortar and pestle and transferred into stainless steel grinding jars of 5 mL (± 200 mg physical mixture) with three 10 mm stainless steel beads. The samples were cryo-milled by applying the following conditions: a pre-cooling period of 1 min at 5 Hz and a cryo-milling period of 3 h at 25 Hz (liquid nitrogen: −196 °C). To prevent overheating, the 3 h interval was evenly spread over six intervals of 30 min at 25 Hz, alternated with an oscillation period of 5 min at 5 Hz. The resulting powder samples were stored at −28 °C in the presence of phosphorus pentoxide until further analysis (*i.e.* solid-state characterization and determination of drug release kinetics).

2.5. Solid-state characterization

2.5.1. Modulated differential scanning calorimetry (mDSC)

A Q2000 mDSC (TA Instruments, Leatherhead, UK), equipped with a refrigerated cooling system (RCS90) and a dry nitrogen purge with a flow rate of 50 mL/min, was used. Calibration for temperature, enthalpy and heat capacity was carried out using indium and sapphire standards. The following parameters were applied: a linear heating rate of 2 °C/min combined with a modulation amplitude of 0.212 °C and a period of 40 s. Approximately 1–3 mg of the sample were accurately weighed into aluminum DSC pans (TA Instruments, Zellik, Belgium). For the samples containing ITC, a heating procedure ranging from 0 °C to 200 °C was applied. For samples with FFB, the heating procedure ranged from −40 °C to 100 °C (for FFB-PEtOx systems), to 120 °C (for FFB-PVP-VA systems) and to 170 °C (for FFB-PVP and FFB-HPMC systems). DSC thermograms were analysed using Universal Analysis software (Version 5.5, TA Instruments, Leatherhead, UK).

2.5.2. X-ray powder diffraction (XRPD)

XRPD was performed using an X'Pert PRO diffractometer (PANalytical, Almelo, the Netherlands) with a Cu tube (Kα λ = 1.5418 Å) and a generator set at 45 kV and 40 mA. The measurements were executed at room temperature, in transmission mode using Kapton® Polyimide Thin-films (PANalytical, Almelo, the Netherlands). The following experimental settings were selected: continuous scan mode from 4° to 40° 2θ with 0.0167° step size and 400 s counting time. The diffractograms were analysed using X'Pert Data Viewer (Version 1.7, PANalytical, Almelo, The Netherlands).

2.6. In vitro drug release kinetics

In vitro drug release kinetics were explored in simple media with an SR 8 Plus dissolution testing system (Hanson Research, U.S.), thermostatically maintained at 37 °C ± 0.5 °C. Dissolution behavior was assessed according to the United States Pharmacopeia (USP) using the paddle method (USP Apparatus 2) at 75 rpm. The selected solid dispersions (equivalent to a 100 mg itraconazole or fenofibrate dose) were added to the vessels, each containing 400 mL of simple acidic medium. Simple acidic medium for dissolution purposes was obtained by adding 0.5% (w/V) polysorbate 80 to a tenfold dilution of 1 M HCl with purified water and adjusted to pH 1. Drug release was monitored in this medium for 1 h, then a pH shift was performed (with the aim of reaching a pH value of 6.8) by adding approximately 100 mL of an alkaline solution, consisting of 0.25 M $Na_3PO_4{\cdot}12H_2O$ in purified water. Drug release in this neutral environment was monitored subsequently for 4 h. At predetermined time points, 1.5 mL of sample was withdrawn and centrifuged for 7 min at 14,680*g* with an Eppendorf centrifuge 5424 (Hamburg, Germany). The supernatant was filtered through presaturated PTFE filters (0.2 μm) and subsequently fivefold diluted with mobile phase for HPLC analysis. All experiments were performed in triplicate. After each sampling, the volume of the vessel was refilled with 1.5 mL pure medium. Quantification of drug concentrations was done with HPLC using the previously developed and validated methods.

2.7. Statistical analysis

Solubility data were statistically analysed with one-way ANOVA combined with post-hoc t-tests, adjusted with the Bonferroni correction for multiple testing, in order to conclude whether the resulting solubility values of ITC/FFB in presence of the different polymers significantly differ ($p < 0.01$) from the solubility value of the drug in pure medium. Data from the supersaturation experiments were statistically analysed with one-way ANOVA combined with post-hoc t-tests, adjusted with the Bonferroni correction for multiple testing in order to state whether SF in presence of different polymers significantly differ ($p < 0.01$) from SF of pure medium. Finally, data obtained from the *in vitro* dissolution tests were statistically analysed with one-way ANOVA (*i.e.* based on normalized AUC values, $p < 0.05$).

3. Results and discussion

In order to make a clear statement about the potential of PEtOx as ASD carrier in comparison to well-known carriers, a systematic approach is implemented. First, equilibrium solubility values of both drugs are determined in absence and presence of the different polymers (Section 3.1), followed by supersaturation experiments (Section 3.2). In a next step, ASDs are manufactured and for each formulation and each manufacturing technique the highest possible drug loading that still results in a one phase amorphous system is established (Section 3.3). Finally, these highest possible drug loading formulations are evaluated for their pharmaceutical performance by *in vitro* dissolution testing (Section 3.4).

3.1. Solubility experiments

Equilibrium solubility values of ITC and FFB, either in absence or presence of polymer, are graphically depicted in Fig. 1. As can be seen, the results of the solubility experiments with ITC clearly demonstrate higher equilibrium solubility values in acidic medium compared to neutral medium. This is attributed to protonation since ITC is a weak base (*i.e.* with p*K*a values of 2.2 and 3.1, corresponding to the triazole and piperazine function, respectively) [9]. Data of the solubility experiments conducted in simple media illustrate that solubility values of ITC were consistently higher in the presence of a polymer. Moreover, in some cases, statistically significant increases in solubility values were observed. For biorelevant media, in contrast, the influence of the polymers on the solubility was less clear and in most cases the solubility values slightly decreased when polymers were present. However, these values did not significantly differ from the values obtained in pure media. Higher solubility of ITC in simple acidic media compared to biorelevant acidic media and similar solubility values for simple and biorelevant neutral media can possibly be attributed to pH effects since the pH of simple media (pH = 1 for acidic simple media, pH = 6.8 for neutral simple media) slightly differ from the pH of biorelevant media (pH = 1.6 for FaSSGF and pH = 6.5 for FaSSIF).

The results of the solubility experiments with the non-ionizable FFB (see Fig. 1C–D) show pH independent values with respect to simple media. The upward trend in equilibrium solubility values (simple media < FaSSGF < FaSSIF) can be explained by the presence of solubilizing effects due to micellar solubilization, which is more pronounced in FaSSIF than in FaSSGF. It can be noted that FFB is more prone to the solubilizing effects of the biorelevant media when

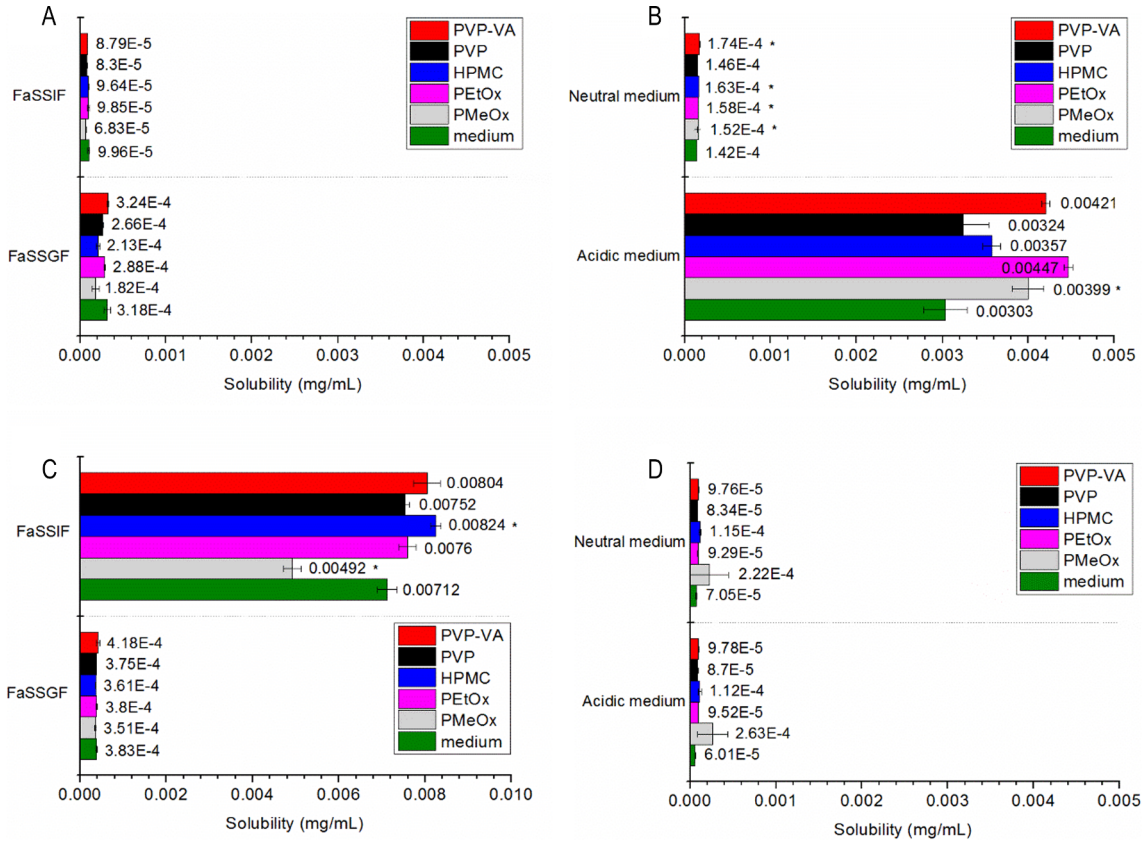

Fig. 1. Average equilibrium solubility values of ITC (in mg/mL) in the absence (in green)/presence of polymers, both in acidic and neutral biorelevant media (A) and acidic and neutral simple media (B). Average equilibrium solubility values of FFB (in mg/mL) in the absence (in green)/presence polymers, both in acidic and neutral biorelevant media (C) and acidic and neutral simple media (D). Values with * indicate solubility values that significantly differ from the solubility value in pure medium ($p < 0.01$). (For interpretation of the references to colour in this figure legend, the reader is referred to the web version of this article.)

compared to ITC, which is probably due to the 'grease ball' character of FFB (=hydrophobic) opposed to the 'brick dust' property of ITC (=strong crystal lattice). As for ITC, experiments conducted in simple media indicate that FFB solubility values were consistently higher in the presence of a polymer, although not statistically significant. The influence of the polymers on solubility was less clear in biorelevant media.

Evaluating the solubility data, it is indeed difficult to distinguish between the different polymers, let alone to make a statement about the potential of PEtOx as ASD carrier.

3.2. Supersaturation experiments

Based on the obtained solubility values, supersaturation experiments were carried out starting from a DS of 20, as applied in previous research [24]. Time-concentration profiles of supersaturation experiments with ITC in biorelevant media are illustrated in Fig. 2 as a representative example. Note that only the solubility of ITC in pure media is depicted since these values do not significantly differ from the values obtained in presence of polymer. However, SF are calculated according to [Eq. (1)], thereby using AUC values based on solubility values in presence of polymer. An overview of the SF for the two compounds in the various media is provided in Table 1. It can be concluded that the polymers exerted little to no effect to inhibit the precipitation of ITC or FFB when compared to SF in pure media. The phenomenon of drug supersaturation in pure media has been reported in literature for ITC. Bevernage et al. observed supersaturation of ITC in human gastric fluids without inclusion of precipitation inhibitors, which was ascribed to charge repulsion. However, the authors state that this repulsion cannot be invoked as the main determinant for supersaturation stability of weakly basic compounds and can also not explain the observed effect in neutral medium, let alone for FFB. The rationale behind this observed effect thus still remains elusive [24]. It is hypothesized that another experimental procedure may lead to more pronounced differences between the different polymers. For example, Tonnis et al. pointed out that differences can be seen in drug supersaturation depending on whether the polymer is pre-dissolved in the media or co-dissolved in the drug solution [25]. Co-dissolved polymers can lead to the formation of drug-polymer interactions (*e.g.* pre-formed hydrogen bonds) and hence better resist the interaction disruption upon addition to the aqueous medium. The method applied in this research encompasses pre-dissolved polymers in the media, possibly inducing weaker drug-polymer interactions (*i.e.* minimal H-bonding) and less supersaturation effects, thereby making it more difficult to observe differences. In conclusion it can be formulated that even though supersaturation experiments do not allow to distinguish between the different polymers, they do reveal that PEtOx is able to maintain supersaturation of ITC and FFB to the same extent as the commercially available polymers. Due to the similar outcomes observed for PMeOx and PEtOx and the limited availability of PMeOx, only PEtOx was withheld for ASD manufacturing.

3.3. ASD manufacturing: Determination of highest possible drug loading

A drug loading screening (most often with 35% drug loading as starting point) was performed for each formulation and each manufacturing process, in order to define the highest possible drug loading that still results in a single phase amorphous system. Noteworthy, drug loadings are based on weight and hence refer to the drug weight fraction in the formulation. Given the potential physical stability issues of ASDs, relatively low drug loadings are utilized in general (*ca.* 30–35%).

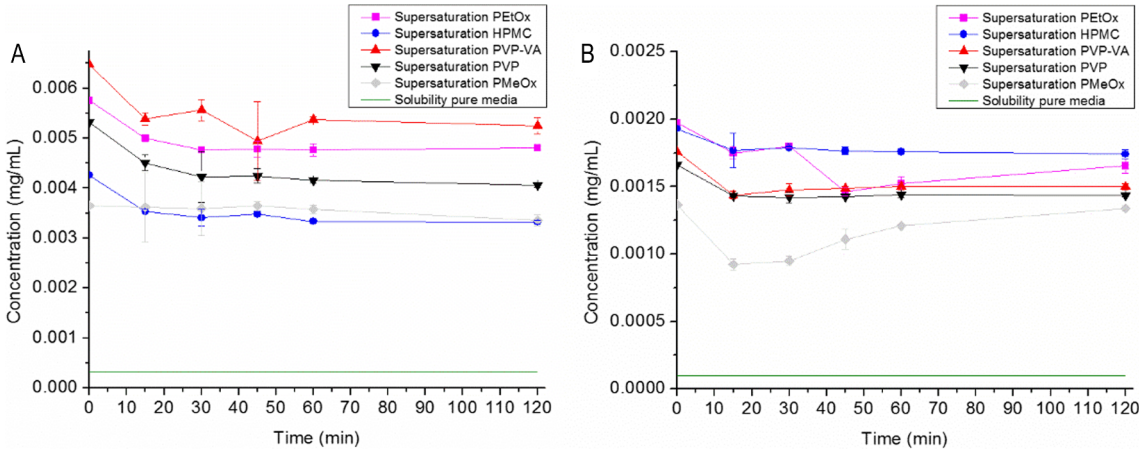

Fig. 2. Time-concentration profiles of supersaturation experiments with ITC in (A) acidic biorelevant medium and in (B) neutral biorelevant medium. The reference solubility of pure ITC is found in green. (For interpretation of the references to colour in this figure legend, the reader is referred to the web version of this article.)

Table 1
Average supersaturation factors (SF) ± standard deviation. Values indicated with * indicate SF that significantly differ from the SF of pure medium ($p < 0.01$).

Itraconazole			
Acidic medium		***Neutral medium***	
Pure medium	18.3 ± 0.3	Pure medium	3.76 ± 0.02
PVP	17.9 ± 0.08	PVP	3.35 ± 0.08
PVPVA	17.5 ± 0.7	PVPVA	3.9 ± 0.4
HPMC	17.0 ± 0.9	HPMC	4.47 ± 0.05*
PEtOx	16.5 ± 1.6	PEtOx	3.8 ± 0.4
PMeOx	17.7 ± 0.5	PMeOx	3.05 ± 0.12*
FaSSGF		***FaSSGF + FaSSIF***	
Pure medium	17.1 ± 0.3	Pure medium	17.2 ± 0.3
PVP	15.7 ± 0.3*	PVP	17.3 ± 0.2
PVPVA	16.4 ± 0.3	PVPVA	17.1 ± 0.2
HPMC	15.9 ± 0.14*	HPMC	18.2 ± 0.13*
PEtOx	16.7 ± 0.2	PEtOx	16.3 ± 0.4
PMeOx	19.4 ± 0.4*	PMeOx	17.2 ± 0.12
Fenofibrate			
Acidic medium		***Neutral medium***	
Pure medium	5.5 ± 0.9	Pure medium	4.4 ± 0.3
PVP	3.6 ± 0.5	PVP	2.6 ± 0.2*
PVPVA	4.9 ± 0.5	PVPVA	2.4 ± 0.2*
HPMC	4.0 ± 0.3	HPMC	2.5 ± 0.2*
PEtOx	3.5 ± 0.3	PEtOx	1.88 ± 0.06*
PMeOx	0.95 ± 0.10	PMeOx	0.646 ± 0.010*
FaSSGF		***FaSSGF + FaSSIF***	
Pure medium	4.8 ± 0.2	Pure medium	1.59 ± 0.04
PVP	3.32 ± 0.07*	PVP	1.6 ± 0.2
PVPVA	3.21 ± 0.03*	PVPVA	1.8 ± 0.2
HPMC	3.57 ± 0.07	HPMC	1.60 ± 0.04
PEtOx	3.28 ± 0.02*	PEtOx	1.53 ± 0.09
PMeOx	3.77 ± 0.18*	PMeOx	3.8 ± 1.1

Nevertheless, it is of utmost importance to obtain drug loadings as high as possible, aiming to lower the pill burden and/or reduce the dosage size to enhance therapeutic compliance of the patient.

3.3.1. Spray drying

Firstly, the same drug loading of ITC was spray dried in combination with each of the four polymers. Applying a 35% drug loading resulted in a different phase behavior for the different formulations (see Fig. 3). Solid-state characterization of the spray dried starting formulations revealed that drug loadings can be increased further for ITC-35-PEtOx and ITC-35-HPMC formulations, since mDSC thermograms show a single T_g indicating a one phase amorphous system. In one phase amorphous systems, the T_g is most often located between the T_g of the pure amorphous drug and the one from the polymer. While in Fig. 4, the drug increasing approach is only described for spray dried ITC-PEtOx systems, the same principle was applied for all drug-polymer combinations, irrespective of the manufacturing technique used, of which the starting formulation is characterized by both a single T_g and halo pattern. New formulations with higher drug loadings were prepared, using consecutive steps of 5%. Since a melting point appears for the ITC-45-PEtOx formulation, ITC-40-PEtOx is selected as highest possible drug loading ASD formulation. Importantly, from the melting events indicating crystallinity, it can be noted that the melting points of ITC slightly differ from the one of the pure drug. It can be argued whether the melting events correspond to the melting of the most stable ITC polymorph (*i.e.* 168 °C), subject to melting point depression, or to the melting of the metastable itraconazole *Form II* polymorph (*i.e.* 155 °C) [26,27].

As clearly seen in Fig. 3, in contrast, the drug loading had to be lowered for the ITC-35-PVP-VA formulation because of amorphous-amorphous phase separation (which in turn can culminate in crystallinity) indicated by two T_g's in the reversing heat flow (RHF) of the mDSC thermogram, corresponding to a drug-rich and polymer-rich phase. For the ITC-35-PVP formulation, drug loading also had to be lowered, given the endothermal peak signaling crystallinity. In addition to crystallinity, interestingly, the mDSC thermogram (Fig. 3A) of ITC-35-PVP indicates a T_g at approximately 60 °C and two endothermal peaks at temperatures 74 °C and 90 °C. These events are attributed to a chiral nematic mesophase of ITC, as described by Six et al. [26]. This mesophase, also known as the liquid crystalline phase, is an additional phase that can be identified between the anisotropic, long-range ordered solid state and the isotropic, short-range ordered liquid state. Since only one phase amorphous systems are being sought in this research, drug loading had to be lowered for the ITC-PVP formulation. Formulations with lower drug weight fractions were prepared by consecutive steps of 5% and solid-state characterization outcomes are depicted in Fig. 5, which serves as an example for all drug lowering approaches applied in this research. Finally, the drug loading screening of the spray dried formulations resulted in highest drug weight fractions of 20% for ITC-PVP, 30% for ITC-PVP-VA and 40% for both ITC-PEtOx and ITC-HPMC drug-polymer combinations, as outlined in Table 2. Interestingly, for spray dried formulations, an equally high drug loading can be achieved with PEtOx as with HPMC, the polymer which is currently used for commercialization of ITC (*i.e.* Sporanox® and Onmel™).

XRPD diffractograms of all spray dried starting formulations show

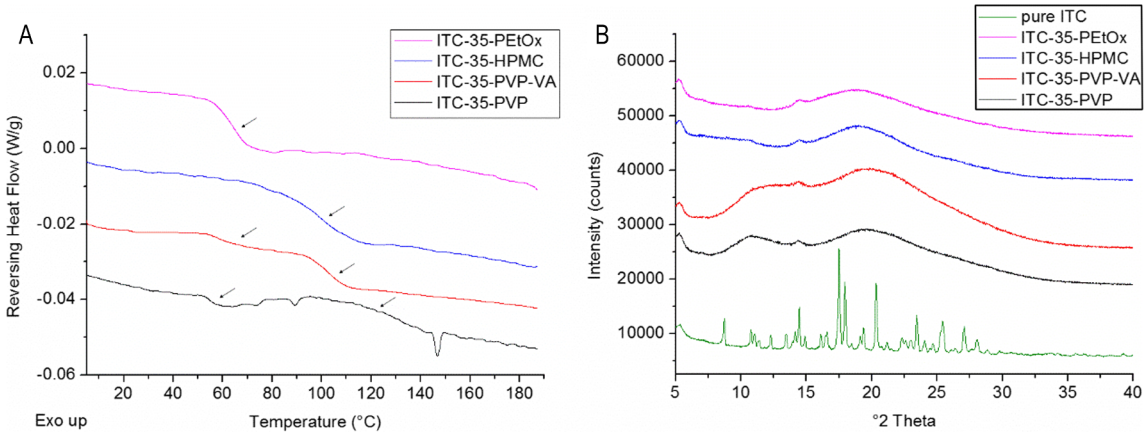

Fig. 3. (A) mDSC thermograms of 35% ITC spray dried formulations with different carriers: PVP (black), PVP-VA (red), HPMC (blue) and PEtOx (pink). The arrows indicate the positions of the T_gs. The reversing heat flow (RHF) signals are shown as arbitrary units. Noteworthy, the thermogram of the spray dried 35% ITC-PVP system indicates the formation of a chiral nematic mesophase. (B) Corresponding XRPD diffractograms and the diffractogram of pure ITC (green) as comparison. The intensities are shown as arbitrary units. (For interpretation of the references to colour in this figure legend, the reader is referred to the web version of this article.)

an amorphous halo (see Fig. 3B). The small observable peaks just before 15° are due to Kapton Polyimide Film since XRPD measurements are conducted in transmission mode. Hence, mDSC was found to be decisive in the drug loading screening of spray dried ITC since no diffraction peaks could be observed for any formulation, even if mDSC revealed some crystallinity. The higher sensitivity of mDSC compared to XRPD can serve as an explanation for this observation. It is thus hypothesized that too few crystals are present in the sample to be detected with XRPD or that the length of coherence is reduced. Moreover, amorphous-amorphous phase separation can only be distinguished from a single amorphous system with mDSC, because XRPD shows an amorphous halo in both cases. Despite XRPD shortcomings, it is still indispensable to implement both mDSC and XRPD as complementary solid-state analytical techniques to provide a comprehensive characterization of the prepared ASDs. A recent paper of Dedroog et al. [28] pointed out that properties of the ASD sample can alter when applying a heating procedure during mDSC. Even a small amount of heat can incite dissolution of the API in the polymer matrix, resulting in mDSC profiles which do not show crystallinity in contrast with the corresponding diffractograms containing diffraction peaks. A similar case was also reported by Bikiaris et al., further highlighting the importance of combining both techniques [29]. An additional problem associated to the use of mDSC as stand-alone technique for solid-state characterization is the overlap of solvent evaporation with recrystallization or melting events, which is often the case for drugs with low melting points (*e.g.* FFB, T_m = 80 °C).

In a next step, the same drug loading screening approach was applied for FFB. FFB, with a starting drug weight fraction of 35%, was spray dried in combination with each of the four polymers and resulted in a drug lowering approach for all formulations due to melting events on the mDSC thermograms and Bragg peaks in the corresponding diffractograms. As reported in Table 2, lowering the drug loadings resulted in the determination of the highest possible drug loading for each formulation: 5% for FFB-PVP-VA, 10% for FFB-PEtOx and 20% for FFB-HPMC systems. The spray dried FFB-5-PVP formulation still showed Bragg peaks in its diffractogram and therefore the highest possible drug loading is indicated as “below 5%”. In contrast to spray dried ITC formulations, XRPD was found to be decisive in the determination of the highest possible drug loading for FFB-PVP and FFB-PVP-VA systems. For example, mDSC thermograms of FFB-PVP systems indicated the formation of single T_g amorphous systems as from 25% drug loading, in contrast with their corresponding diffractograms signaling crystallinity. As indicated above, overlap of solvent evaporation with the melting event of FFB can serve as a possible explanation. The other hypothesis, which implies that due to mobility inducement, FFB dissolves in the polymer during heating, may also apply here since the melting event starts at the beginning of the glass transition. It is important to note that, for spray drying of low T_g FFB-PEtOx systems, process parameters were altered in order to obtain a powder. Hence, it could be argued to what extent this resulting drug loading can be compared to those of the

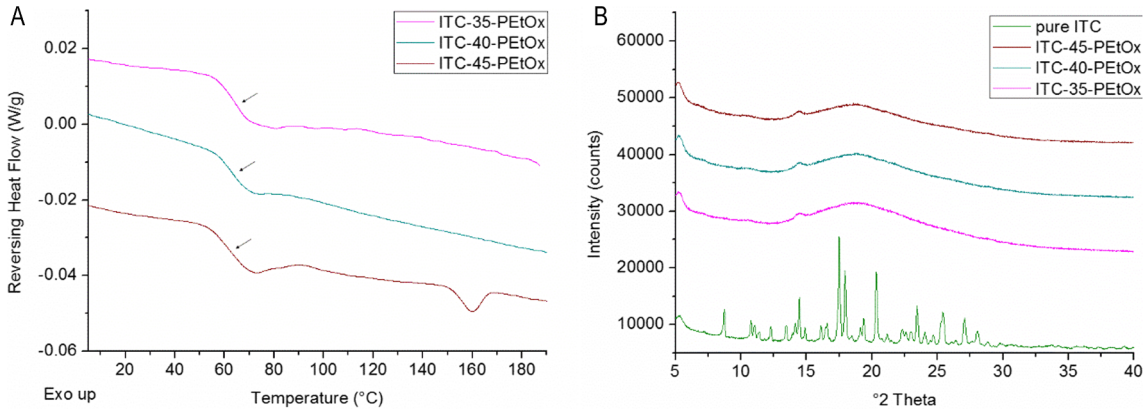

Fig. 4. (A) mDSC thermograms of spray dried ITC-PEtOx systems, increasing the drug loading from 35% to 45% by intermediate steps of 5%. The arrows indicate the positions of the T_gs. The RHF signals are shown as arbitrary units. (B) Corresponding XRPD diffractograms and the diffractogram of pure ITC (green) as comparison. The intensities are shown as arbitrary units. (For interpretation of the references to colour in this figure legend, the reader is referred to the web version of this article.)

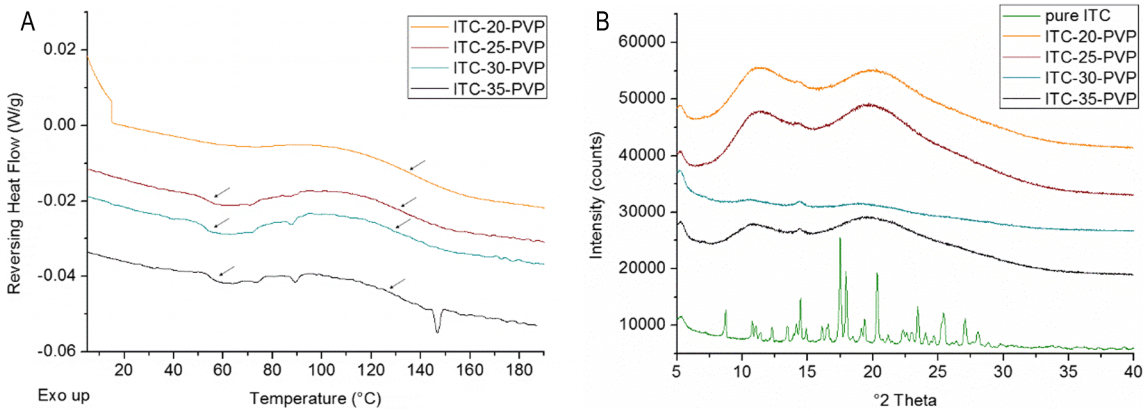

Fig. 5. (A) mDSC thermograms of spray dried ITC-PVP systems, lowering the drug loading from 35% to 20% by intermediate steps of 5%. The arrows indicate the positions of the T_gs. The RHF signals are shown as arbitrary units. (B) Corresponding XRPD diffractograms and the diffractogram of pure ITC (green) as comparison. The intensities are shown as arbitrary units. (For interpretation of the references to colour in this figure legend, the reader is referred to the web version of this article.)

other formulations. The influence of process parameters on the final product properties was, however, not within the aims of this study.

Although the outcome of the drug loading screening is strongly API dependent, it does provide a first proof of the potential of PEtOx for drug formulation purposes. The ease and the speed with which PEtOx dissolves in various solvents offers an additional argument in favor of this polymer.

3.3.2. Hot melt extrusion

A 35% drug loading of ITC was extruded with each of the four polymers but, in contrast to spray drying, resulted in the same phase behavior for all drug-polymer combinations (see Fig. 6). Thermograms of all hot melt extruded starting formulations indicate that one phase amorphous systems were obtained, hence drug loadings were increased. As a result, drug loadings of 35% were obtained for ITC-HPMC and ITC-PVP formulations, 40% for ITC-PEtOx and a value of 50% was reached for ITC-PVP-VA. Noteworthy, crystallinity was induced in ITC-40-PEtOx and ITC-50-PVP-VA systems when the extrudate milling time was increased from 1 min to 3 min, in order to further reduce the particle size (*i.e.* < 355 μm) with a view to *in vitro* dissolution experiments. Therefore, ITC-35-PEtOx and ITC-45-PVP-VA formulations were manufactured and subsequently tested for milling-induced crystallinity. These formulations turned out to be stable and were therefore selected as highest possible drug loading (see Table 2). Evidence on the usefulness of PEtOx as ASD carrier is thus fortified. Moreover, PEtOx can overcome an important limitation of HME thereby entailing the possibility of formulating thermolabile drugs with a low melting point due to its relatively low T_g (*i.e.* 60 °C) in comparison to the T_g of the commercially available polymers (*i.e.* 147 °C for HPMC, 161 °C for PVP and 110 °C for PVP-VA).

As for spray dried ITC formulations, mDSC was found to be decisive in the drug loading screening since all diffractograms show an amorphous halo, irrespective of the drug loading or polymer used. The sharp peak in the diffractogram of hot melt extruded ITC-35-HPMC originates from a crystalline impurity present in the polymer.

Regarding HME of FFB, solid state-characterization of the 35% drug weight fraction systems affirmed that drug loadings had to be lowered. The final drug loadings are represented in Table 2. For hot melt extruded FFB-PVP and FFB-PVP-VA systems, XRPD was found to be decisive in the determination of the highest possible drug loading. In this respect, the hypotheses described for spray dried FFB-PVP and FFB-PVP-VA systems may also apply here.

3.3.3. Cryo-milling

A 35% drug loading of ITC was cryo-milled in combination with each of the four polymers and led to the same phase behavior for all formulations. Thermograms of the cryo-milled starting formulations point out that drug loadings can be increased further (Fig. 7a). For the

Table 2
Overview of the highest possible weight fractions of ITC and FFB, for each formulation and each manufacturing process, that still result in one phase amorphous systems. The factors that determined these drug loadings are indicated as well. *Indicates formulation with altered process parameters.

Itraconazole						
	Spray drying		***Hot melt extrusion***		***Cryo-milling***	
	Drug loading (%)	Determining factor	Drug loading (%)	Determining factor	Drug loading (%)	Determining factor
PVP K30	20	Chiral nematic mesophase	35	Phase separation	50	Crystallinity
PVP-VA 64	30	Phase separation	45	Milling induced crystallinity	45	Phase separation
PEtOx	40	Crystallinity	35	Milling induced crystallinity	40	Crystallinity
HPMC	40	Crystallinity	35	Crystallinity	45	Crystallinity
Fenofibrate						
	Spray drying		***Hot melt extrusion***		***Cryo-milling***	
	Drug loading (%)	Determining factor	Drug loading (%)	Determining factor	Drug loading (%)	Determining factor
PVP K30	< 5	Crystallinity	20	Crystallinity	10	Crystallinity
PVP-VA 64	5	Crystallinity	30	Crystallinity	10	Crystallinity
PEtOx	10*	Crystallinity	30	Crystallinity	5	Crystallinity
HPMC	20	Crystallinity	15	Crystallinity	< 5	Crystallinity

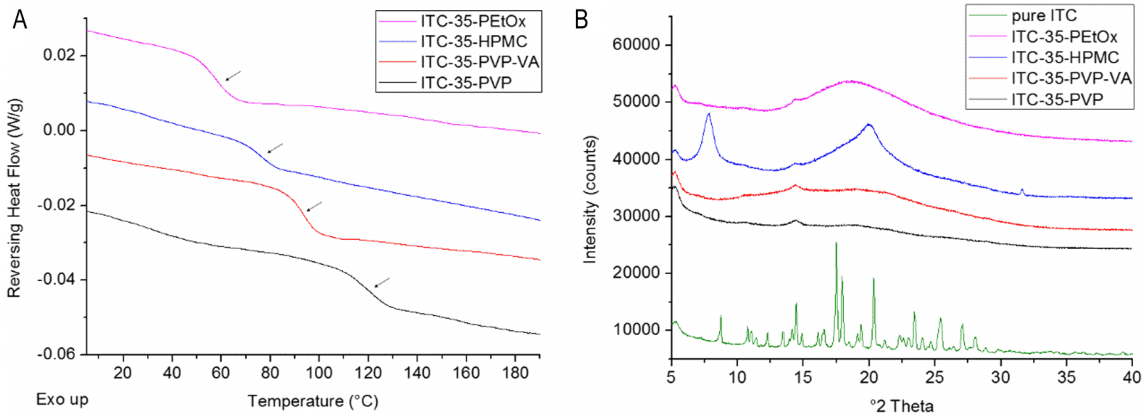

Fig. 6. (A) mDSC thermograms of 35% ITC hot melt extruded formulations with different carriers: PVP (black), PVP-VA (red), HPMC (blue) and PEtOx (pink). The arrows indicate the positions of the T_gs. The RHF signals are shown as arbitrary units. (B) Corresponding XRPD diffractograms and the diffractogram of pure ITC (green) as comparison. The intensities are shown as arbitrary units. The sharp peak in the diffractogram of the ASD with HPMC (blue) originates from a crystalline impurity present in the polymer. (For interpretation of the references to colour in this figure legend, the reader is referred to the web version of this article.)

cryo-milled ITC-PEtOx formulations, the screening resulted in a maximum drug weight fraction of 40% and for the cryo-milled ITC-HPMC and ITC-PVP-VA formulations, a drug loading up to 45% was reached. Even 50% drug weight fraction was obtained for the ITC-PVP formulation, as shown in Table 2. Fascinatingly, for ITC, the highest drug loading for each of the formulations can reproducibly be obtained with cryo-milling, which is still considered as non-conventional nowadays. However, the manufacturing of larger quantities (*e.g.* for *in vitro* dissolution purposes) is time-consuming. In general, Table 2 clarifies that, next to the drug-polymer combination, the applied manufacturing technique is a critical factor for reaching high drug loadings. This is in alignment with some recent findings in literature, which emphasize the importance of the manufacturing technique used [28].

For cryo-milling of FFB-polymer combinations, a starting point of 15% drug loading was applied. The ASD manufacturing and solid-state characterization interplay resulted in determination of highest possible drug loadings, as depicted in Table 2.

3.3.4. Experimental vs theoretical T_g values

For all ITC formulations with 35% drug loading, experimental T_g values were compared to theoretical T_g values. The latter were calculated using the following Gordon-Taylor equation [Eq. (2)]:

$$T_{gmix} = \frac{w_1 * T_{g1} + K * w_2 * T_{g2}}{w_1 + K * w_2} \quad (2)$$

where w represents the weight fraction, T_g the glass transition temperature (absolute T), subscripts 1 and 2 indicate the amorphous compounds with the lowest and highest T_g, respectively and $K \cong \frac{\rho 1 * Tg1}{\rho 2 * Tg2}$ where ρ represents the density of the amorphous compound.

This equation only applies to ideal mixtures, implying that the strength of drug-drug and polymer-polymer interactions are of the same order than that of drug-polymer interactions. Table 3 suggests that the theoretical values, obtained with Eq. (2), serve as a good prediction for the corresponding experimental values. Although the ITC-HPMC system interacts via H-bonds, theoretical T_g values are higher than their experimental counterpart, suggesting stronger drug-drug and/or polymer-polymer interactions compared to the drug-polymer interactions.

3.3.5. T_g widths

For all 35% ITC HME and cryo-milled formulations, mDSC thermograms indicate the formation of a one phase amorphous system. Although a single T_g is detected, it can be interesting at this point to investigate the T_g widths and the AUC of the derivative of the reversing heat flow (AUC Der. RHF). Indeed, the broader the T_g, the more heterogeneous the solid dispersion is and consequently the sooner phase separation and thus crystallization may occur. T_g widths and AUC values are reported for 35% ITC hot melt extruded and cryo-milled formulations and theoretical AUC Der. RHF values and theoretical T_g widths for the formulations were calculated from the values of the pure components assuming simple additivity (see Table 4). The results

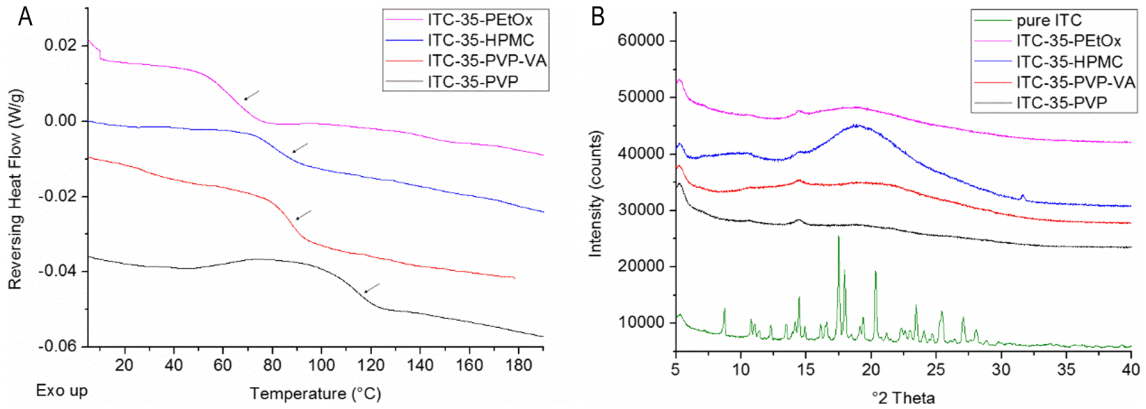

Fig. 7. (A) mDSC thermograms of 35% ITC cryo-milled formulations with different carriers: PVP (black), PVP-VA (red), HPMC (blue) and PEtOx (pink). The arrows indicate the positions of the T_gs. The RHF signals are shown as arbitrary units. (B) Corresponding XRPD diffractograms and the diffractogram of ITC (green) as comparison. The intensities are shown as arbitrary units. The sharp peak in the diffractogram of the ASD with HPMC (blue) originates from a crystalline impurity present in the polymer. (For interpretation of the references to colour in this figure legend, the reader is referred to the web version of this article.)

Table 3
Theoretical T_g values, calculated with the Gordon-Taylor equation, and experimental T_g values for 35% ITC spray dried, hot melt extruded and cryo-milled formulations. Formulations indicated with * were not one phase amorphous systems.

Itraconazole			
Theoretical T_g values (°C)		***Experimental T_g values (°C) - HME***	
ITC-35-PEtOx	60.0	ITC-35-PEtOx (HME)	58.3
ITC-35-HPMC	112.9	ITC-35-HPMC (HME)	77.3
ITC-35-PVP-VA	92.3	ITC-35-PVP-VA (HME)	94.1
ITC-35-PVP	123.5	ITC-35-PVP (HME)	120.8
Experimental T_g values (°C) - SD		***Experimental T_g values (°C) - CM***	
ITC-35-PEtOx (SD)	63.5	ITC-35-PEtOx (CM)	63.8
ITC-35-HPMC (SD)	97.5	ITC-35-HPMC (CM)	77.4
ITC-35-PVP-VA (SD) *	58.1/101.5	ITC-35-PVP-VA (CM)	86.2
ITC-35-PVP (SD) *	55.0/131.1	ITC-35-PVP (CM)	112.9

Table 4
Experimental T_g values, the corresponding T_g widths and areas under curve of the derivative of the reversing heat flow (AUC Der. RHF) for 35% ITC hot melt extruded formulations (upper values), for 35% ITC cryo-milled formulations (lower values) and for the pure components. The last column represents theoretical AUC Der. RHF values and theoretical T_g widths for the formulations, calculated from the values of the pure components.

Itraconazole					
Formulation	***T_g values (°C)***	***T_g width (°C)***	***AUC Der. RHF (W * min/ (g * °C))***	***Theor. AUC Der. RHF (W * min/ (g * °C))***	***Theor. T_g width (°C)***
ITC-35-PVP	120.8	11.0	0.0032	0.0031	10.9
	112.9	14.4	0.0049		
ITC-35-PVP-VA	94.1	8.8	0.0056	0.0029	6.4
	86.2	7.6	0.0038		
ITC-35-HPMC	77.3	14.7	0.0024	0.0020	8.9
	77.4	13.6	0.0037		
ITC-35-PEtOx	58.3	12.1	0.0055	0.0042	8.8
	63.8	13.3	0.0069		
Pure component	***T_g values (°C)***	***T_g width (°C)***	***AUC Der. RHF (W * min/ (g * °C))***		
ITC	60.1	4.9	0.0038		
PVP	169.1	14.2	0.0027		
PVP-VA	108.5	7.2	0.0025		
HPMC	147.3	11.1	0.0011		
PEtOx	63.2	11.0	0.0044		

indicate that the experimental T_g width and corresponding AUC Der. RHF of the ITC-35-PVP hot melt extruded solid dispersion can be well predicted theoretically. For the other formulations, theoretical T_g widths and AUC Der. RHF are systematically lower than their corresponding experimental values, which implies that more heterogeneity is present in the system than would be expected for an ideal mixture.

3.4. *In vitro* drug release kinetics

The formulations with the highest possible drug weight fractions (see Table 2) were selected for pharmaceutical performance test purposes. This is an important criterion to distinguish between the different formulations and manufacturing processes and hence, to give an answer to the key question of this research. For ITC, *in vitro* dissolution was tested for all highest possible drug loading formulations (*i.e.* spray dried, hot melt extruded and cryo-milled formulations) and the resulting time-concentration profiles are shown in Fig. 8(A–C). In contrast, for FFB, pharmaceutical performance was only tested for the highest possible drug loading formulations prepared with HME, due to lack of polymer material for the spray dried and cryo-milled formulations given the low drug loadings. The time-concentration profiles of the *in vitro* dissolution experiment with FFB are depicted in Fig. 8D. For each formulation, the corresponding drug loading is indicated. Noteworthy, after 60 min, the dissolution medium was subject to a pH shift, which explains the rapid precipitation of the weak base ITC from this timepoint on. Solubility values in both acidic and neutral medium are also represented.

The resulting time-concentration profiles, represented in Fig. 8, were statistically analysed with one-way ANOVA based on normalized AUC values before (5–60 min) and after (70–300 min) the pH shift. The AUC values were normalized for the polymer content in order to eradicate the effect of different polymer quantities. Indeed, it is known that relative polymer quantities play a role in the release kinetics of the solid dispersions (*i.e.* a higher polymer weight fraction in the formulation will often result in a better release of the drug) [30]. In a first step, differences between the different formulations, and hence polymers as such, are analysed per manufacturing technique. Secondly, the focus lies on the differences between the manufacturing techniques per formulation. Mean normalized AUC values and the corresponding standard deviations are reported in Table 5.

For ITC spray dried formulations, ANOVA based on normalized AUC (5–60 min) revealed significant differences between the different formulations. It is observed that the formulation with PEtOx shows the highest normalized AUC value for the first hour of the dissolution experiment. ANOVA based on normalized AUC (70–300 min) also shows a significant difference between the different formulations and further demonstrate that the formulation with PEtOx underwent a high driving force for precipitation, resulting in the lowest normalized AUC value for the timeframe after the pH shift. For ITC HME formulations, the ANOVA based on normalized AUC (5–60 min) also illustrates the highest normalized AUC values for the ITC-PEtOx formulation, however not significantly. In addition, no significant differences were observed between the formulations for the 70–300 min timeframe. For ITC cryo-milled formulations, the ANOVA based on normalized AUC (5–60 min) revealed significant differences between the different formulations. However, the highest normalized AUC values were obtained for the formulations with PVP-VA. ANOVA for the 70–300 min period also shows a significant difference between the different formulations and reveals that the precipitation driving force for ITC-PVP-VA is less pronounced. Noteworthy, for all manufacturing techniques, formulations with HPMC obtained the highest normalized AUC values for the timeframe after the pH shift. Despite the fact that the polymers had a limited effect on the solubility and supersaturation in the above-described experiments, the dissolution of ITC from the ASD was significantly improved as compared to the original ITC material. Overall, it can be concluded that PEtOx is able to ensure high drug release, irrespective of the manufacturing technique used.

When focusing on the differences between the manufacturing techniques for each formulation with ITC, ANOVA based on normalized AUC (5–60 min) values encompasses p-values less than 0.05 and hence demonstrates significant differences between the different ASD manufacturing techniques. It can be concluded that the highest normalized AUC values are obtained for all formulations prepared with hot melt extrusion and thus that this manufacturing technique gives rise to the best *in vitro* pharmaceutical performance. For ITC-HPMC and ITC-PEtOx, the ASD preparation methods can be ordered based on pharmaceutical performance: HME > spray drying > cryo-milling. In contrast, for ITC-PVP and ITC-PVP-VA the ranking based on pharmaceutical performance is as follows: HME > cryo-milling > spray drying. ANOVA based on normalized AUC (70–300 min) only demonstrates significant differences for the formulations with PVP and PEtOx and indicates that the highest normalized AUC values are obtained for this timeframe when cryo-milling was used as manufacturing technique.

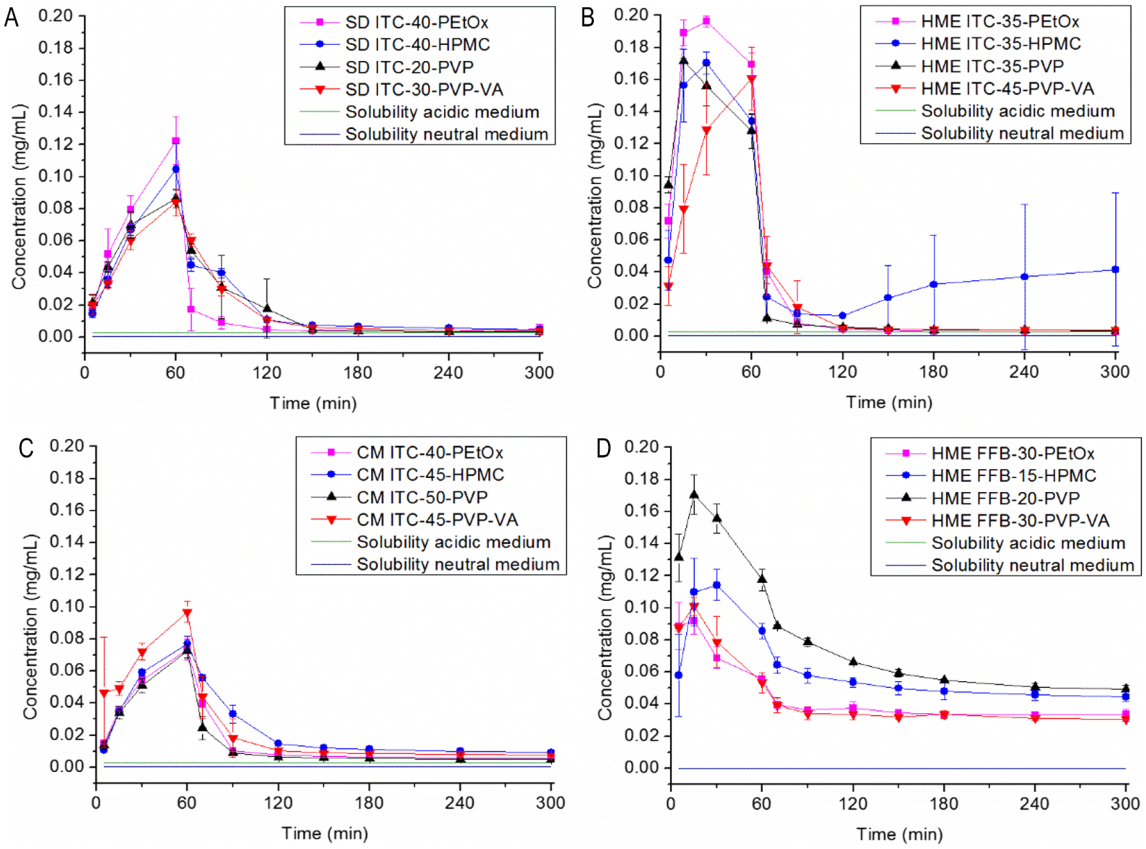

Fig. 8. Drug release profiles of (A) spray dried ITC formulations, (B) hot melt extruded ITC formulations, (C) cryo-milled ITC formulations, (D) hot melt extruded FFB formulations. For each formulation, the corresponding drug loading is indicated. Solubility values of ITC (A–C) and FFB (D) both in acidic (green) and neutral medium (dark blue) are also represented. (For interpretation of the references to colour in this figure legend, the reader is referred to the web version of this article.)

Table 5
Mean normalized AUC values ± standard deviation, resulting from the *in vitro* dissolution experiments of the different ITC and FFB formulations prepared with hot melt extrusion (HME), spray drying (SD) and cryo-milling (CM), before (5–60 min) (*i.e.* upper values) and after (70–300 min) (*i.e.* lower values) the pH shift. P-values of one-way ANOVA analyses are also reported.

Itraconazole

Formulation	*HME*	*SD*	*CM*	*ANOVA*
ITC-PVP	12.4 ± 0.7	4.4 ± 0.3	5.4 ± 0.4	p = 3E−06
	1.7 ± 0.3	3.1 ± 0.8	3.1 ± 0.3	p = 0.03
ITC-PVP-VA	12 ± 2	4.5 ± 0.4	7.1 ± 0.2	p = 0.002
	3.1 ± 0.9	3.51 ± 0.19	4.6 ± 1.1	p = 0.15
ITC-HPMC	12.4 ± 0.4	6.0 ± 0.6	5.4 ± 0.2	p = 1.8E−06
	10 ± 9	4.58 ± 0.17	6.5 ± 0.5	p = 0.5
ITC-PEtOx	14.9 ± 0.17	7.3 ± 0.8	4.7 ± 0.2	p = 8E−07
	1.9 ± 0.2	2.0 ± 0.5	3.16 ± 0.12	p = 0.003
ANOVA	p = 0.07	p = 0.0007	p = 0.00004	
	p = 0.2	p = 0.001	p = 0.0006	

Fenofibrate

Formulation	*HME*
FFB-PVP	10.3 ± 0.6
	17.0 ± 0.4
FFB-PVP-VA	6.7 ± 0.2
	10.7 ± 0.4
FFB-HPMC	6.2 ± 1.1
	13.4 ± 1.0
FFB-PEtOx	6.3 ± 0.6
	11.4 ± 0.6
ANOVA	p = 0.0002
	p = 1.1E-05

For FFB, pharmaceutical performance was only tested for the highest possible drug loading formulations prepared with HME and hence statements about differences between the manufacturing techniques cannot be made. As reported in Table 5, ANOVA based on normalized AUC values, for both timeframes, revealed that the FFB-PVP formulation performed significantly better than the other formulations.

In general, with respect to PEtOx, these data highlight its potential for drug delivery purposes. Although in some cases highest mean normalized AUC values are obtained when PEtOx was used as carrier, its overall performance is comparable to the well-known, commercially available carriers.

Furthermore, it can be noted that the mean normalized AUC values for the timeframe after the pH shift are much higher for FFB formulations, compared to ITC formulations. This can be explained by the non-ionizable character of FFB compared to the weak base ITC, that precipitated due to the increase in pH.

Nevertheless, the reader should keep in mind that statistically significant differences from *in vitro* experiments do not necessarily imply relevance *in vivo*. In addition, caution is required when generalizing the data, since statistical power is limited due to small sample sizes (n = 3).

Since physical stability tests were not within the aim of this study, they form an interesting topic and necessity for future research, given the relatively low T_g of PEtOx. Together with investigation of possible drug-polymer interactions (*i.e.* possible van der Waals interactions between PEtOx and ITC/FFB), a more comprehensive outline of the potential of PEtOx can be achieved.

4. Conclusions

In this study, the potential of PEtOx as ASD carrier was investigated by means of a benchmark approach with HPMC, PVP K30 and PVP-VA

64. For this purpose, ITC and FFB were selected as BCS class II model drugs. The four polymers were able to increase equilibrium solubility values of both ITC and FFB in simple media and showed a comparable precipitation inhibition capacity in the supersaturation experiments. In order to thoroughly elaborate their capability as carrier for ASDs, three manufacturing techniques were implemented (*i.e.* spray drying, hot melt extrusion and cryo-milling) in order to cover all three manufacturing categories. For each formulation and each manufacturing technique, a drug loading screening was performed in order to determine the highest possible drug loading that still results in a one phase amorphous system. This screening led to the conclusion that ASDs with acceptable drug loadings can be manufactured with PEtOx as carrier, irrespective of the manufacturing technique used, and thus provides proof of the potential of PEtOx for drug formulation purposes. Although in most cases similar results were obtained for the four polymers, PEtOx offers some additional benefits. The ease and speed with which PEtOx dissolves in various solvents serves as a time-saving advantage within the spray drying process. Moreover, the process temperature during HME can be markedly lowered due its relatively low T_g, thereby entailing the possibility of formulating thermolabile drugs. Finally, pharmaceutical performance of the different formulations was tested and revealed that PEtOx can ensure high drug release, irrespective of the manufacturing technique used. When focusing on the distinct manufacturing techniques, it can be concluded that HME gives rise to the best *in vitro* pharmaceutical performance. Overall, the hereby reported data substantiate the potential of PEtOx as ASD carrier. Despite the promising data collected for PEtOx, its widespread use as a carrier for ASDs is limited by the lack of regulatory approval. Today, FDA approval for PEtOx is still limited to its use as an adhesive in food packaging. However, the recent commercial availability of high quality PEtOx and the current involvement of a PEtOx derivative in clinical trials predict an exciting future for this polymer in the biomedical arena.

References

[1] C.A. Lipinski, F. Lombardo, B.W. Dominy, P.J. Feeney, Experimental and computational approaches to estimate solubility and permeability in drug discovery and development settings, Adv. Drug Deliv. Rev. 46 (2001) 3–26.

[2] A. Singh, Z.A. Worku, G. Van den Mooter, Oral formulation strategies to improve solubility of poorly water-soluble drugs, Expert Opin. Drug Deliv. 8 (10) (2011) 1361–1378.

[3] L.Z. Benet, The role of BCS (Biopharmaceutics Classification System) and BDDCS (Biopharmaceutics Drug Disposition Classification System) in drug development, J. Pharm. Sci. 102 (2013) 34–42.

[4] S. Janssens, G. Van den Mooter, Review: physical chemistry of solid dispersions, J. Pharm. Pharmacol. 61 (12) (2009) 1571–1586.

[5] G. Van den Mooter, The use of amorphous solid dispersions: A formulation strategy to overcome poor solubility and dissolution rate, Drug Discov. Today Technol. 9 (2012) e79–e85.

[6] T. Van Duong, G. Van den Mooter, The role of the carrier in the formulation of pharmaceutical solid dispersions. Part II: amorphous carriers, Expert Opin. Drug Deliv. 13 (12) (2016) 1681–1694.

[7] S. Marques, B. Sarmento, Amorphous solid dispersions : Rational selection of a manufacturing process, Adv. Drug Deliv. Rev. 100 (2016) 85–101.

[8] T. Filo Vasconcelos, B. Sarmento, P. Costa, Solid dispersions as strategy to improve oral bioavailability of poor water soluble drugs, Drug Discov. Today 12 (23) (2007) 1068–1075.

[9] T. Pas, A. Struyf, B. Vergauwen, G. Van den Mooter, Ability of gelatin and BSA to stabilize the supersaturated state of poorly soluble drugs, Eur. J. Pharm. Biopharm. 131 (2018) 211–223.

[10] K. Hrovat, Methods of amorphization and investigation of the amorphous state, Acta Pharm. 63 (2013) 305–334.

[11] N. Kang, J. Lee, J.N. Choi, C. Mao, E.H. Lee, Drug Development and Industrial Pharmacy Cryomilling-induced solid dispersion of poor glass forming/poorly water-soluble mefenamic acid with polyvinylpyrrolidone K12, Drug Dev. Ind. Pharm. 41 (6) (2015) 978–988.

[12] G. Van den Mooter, I. Weuts, T. De Ridder, N. Blaton, Evaluation of Inutec SP1 as a new carrier in the formulation of solid dispersions for poorly soluble drugs, Int. J. Pharm. 316 (2006) 1–6.

[13] S.V. Jermain, C. Brough, R.O.W. Iii, Amorphous solid dispersions and nanocrystal technologies for poorly water-soluble drug delivery – An update, Int. J. Pharm. 535 (2017) 379–392.

[14] B. Claeys, A. Vervaeck, C. Vervaet, J.P. Remon, R. Hoogenboom, B.G. De Geest, Poly (2-ethyl-2-oxazoline) as Matrix Excipient for Drug Formulation by Hot Melt Extrusion and Injection Molding, Macromol. Rapid Commun. 33 (2012) 1701–1707.

[15] H. Fael, C. Ràfols, A.L. Demirel, Poly(2-Ethyl-2-Oxazoline) as an Alternative to Poly (Vinylpyrrolidone) in Solid Dispersions for Solubility and Dissolution Rate Enhancement of Drugs, J. Pharm. Sci. 107 (9) (2018) 2428–2438.

[16] E. Vlassi, A. Papagiannopoulos, S. Pispas, Amphiphilic poly(2-oxazoline) copolymers as self-assembled carriers for drug delivery applications, Eur. Polym. J. 88 (2017) 516–523.

[17] M. Glassner, M. Vergaelen, R. Hoogenboom, Poly(2-oxazoline)s: A comprehensive overview of polymer structures and their physical properties, Polym. Int. 67 (1) (2018) 32–45.

[18] V.R. De La Rosa, Poly(2-oxazoline)s as materials for biomedical applications, J. Mater. Sci. - Mater. Med. 25 (5) (2014) 1211–1225.

[19] E. Rossegger, V. Schenk, F. Wiesbrock, Design strategies for functionalized poly(2-oxazoline)s and derived materials, Polymers (Basel). 5 (3) (2013) 956–1011.

[20] B. Verbraeken, B.D. Monnery, K. Lava, R. Hoogenboom, The chemistry of poly(2-oxazoline)s, Eur. Polym. J. 88 (2017) 451–469.

[21] T. Lorson, M.M. Lübtow, E. Wegener, M.S. Haider, S. Borova, D. Nahm, et al., Poly (2-oxazoline)s based biomaterials: A comprehensive and critical update, Biomaterials 178 (2018) 204–280.

[22] R.W. Moreadith, T.X. Viegas, M.D. Bentley, J.M. Harris, Z. Fang, K. Yoon, et al., Clinical development of a poly(2-oxazoline) (POZ) polymer therapeutic for the treatment of Parkinson's disease – Proof of concept of POZ as a versatile polymer platform for drug development in multiple therapeutic indications, Eur. Polym. J. 88 (2017) 524–552.

[23] B.D. Monnery, V.V. Jerca, O. Sedlacek, B. Verbraeken, R. Cavill, R. Hoogenboom, Defined high molar mass poly(2-oxazoline)s, Angew Chemie - Int Ed. 57 (47) (2018) 15400–15404.

[24] J. Bevernage, B. Hens, J. Brouwers, J. Tack, P. Annaert, P. Augustijns, Supersaturation in human gastric fluids, Eur. J. Pharm. Biopharm. 81 (1) (2012) 184–189.

[25] W. Tonnis, S. Wang, F. Qian, Y. Pui, H. Chen, Y. Chen, et al., Polymer-mediated drug supersaturation controlled by drug-polymer interactions persisting in an aqueous environment, Mol. Pharm. 16 (1) (2019) 205–213.

[26] K. Six, G. Verreck, J. Peeters, K. Binnemans, H. Berghmans, P. Augustijns, et al., Investigation of thermal properties of glassy itraconazole: identification of a monotropic mesophase, Thermochim. Acta 175–81 (2001).

[27] S. Zhang, T.W.Y. Lee, A.H.L. Chow, Crystallization of itraconazole polymorphs from melt, Cryst. Growth Des. 16 (7) (2016) 3791–3801.

[28] S. Dedroog, C. Huygens, G. Van den Mooter, Chemically identical but physically different: A comparison of spray drying, hot melt extrusion and cryo-milling for the formulation of high drug loaded amorphous solid dispersions of naproxen, Eur. J. Pharm. Biopharm. 135 (2019) 1–12.

[29] D. Bikiaris, G.Z. Papageorgiou, A. Stergiou, E. Pavlidou, E. Karavas, F. Kanaze, et al., Physicochemical studies on solid dispersions of poorly water-soluble drugs: Evaluation of capabilities and limitations of thermal analysis techniques, Thermochim. Acta 439 (2005) 58–67.

[30] V. Bhardwaj, N.S. Trasi, D.Y. Zemlyanov, L.S. Taylor, Surface area normalized dissolution to study differences in itraconazole-copovidone solid dispersions prepared by spray-drying and hot melt extrusion, Int. J. Pharm. 540 (1–2) (2018) 106–119.